

Flow of Newtonian Fluid in Non-Uniform Tubes with Application to Renal Flow: A Numerical Study

P. Muthu* and Tesfahun Berhane

*Department of Mathematics, National Institute of Technology, Warangal,
Warangal 506004, India*

Received 21 October 2010; Accepted (in revised version) 18 February 2011

Available online 9 September 2011

Abstract. In this paper, a numerical method employing a finite difference technique is used for an investigation of viscous, incompressible fluid flow in a tube with absorbing wall and slowly varying cross-section. The effect of fluid absorption through permeable wall is accounted by prescribing flux as a function of axial distance. The method is not restricted by the parameters in the problem such as wave number, permeability parameter, amplitude ratio and Reynolds number. The effects of these parameters on the radial velocity and mean pressure drop is studied and the results are presented graphically. Comparison is also made between the results obtained by perturbation method of solution and present approach.

AMS subject classifications: 76Z05, 92C10

Key words: Non-uniform tube, renal flow, Takabatake finite difference scheme.

1 Introduction

The process of reabsorption plays a major role during urine formation in kidneys as 98 percent of glomerular filtrate gets reabsorbed during its passage through renal tubules. Kidneys excrete most of the end products of body metabolism and they control concentrations of most of the constituents of body fluids. The basic functional unit of kidney is nephron. Each kidney contains over a million tiny units (of nephrons), all similar in structure and function. Each nephron functions independently and in most instances it is sufficient to study the function of nephron to understand the mechanism of kidney in terms of mathematical models. In nephrons, the portion after the Bowman's capsule is called proximal convoluted tubule, which is narrower than rest of the tube and non-uniform in nature. It is the place where most of useful substances, like water, glucose and electrolytes are reabsorbed back into the plasma and unwanted

*Corresponding author.

URL: <http://www.nitw.ac.in/nitwnew/facultypage.aspx?didno=9&fidno=622>

Email: snklpm@rediffmail.com (P. Muthu), tesfahunb2002@yahoo.com (T. Berhane)

substances pass into urine. Thus it is of interest to study the flow in proximal tubule using mathematical models.

Study of viscous fluid flow in channels of varying cross section with permeable wall is significant because of its applications to both physiological and engineering flow problems. The flow of fluid in a renal tubule has been studied by various authors. Macey [1] formulated the problem as the flow of an incompressible viscous fluid through a circular tube with linear rate of reabsorption at the wall. Whereas, Kelman [2] found that the bulk flow in the proximal tubule decays exponentially with the axial distance. Then, Macey [3] used this condition to solve the equations of motion and mentioned that the longitudinal velocity profile is parabolic and the drop in mean pressure is proportional to the mean axial flow. Marshall and Trowbridge [4] and Palatt et al. [5] used physical conditions existing at the rigid permeable tube instead of prescribing the flux at the wall as a function of axial distance.

The representation of a proximal tubule as a uniform tube with constant wall permeability is obviously an idealization. Radhakrishnamacharya et al. [6] considered a non-uniform geometry to model renal tubule while the previous studies considered it uniform. They made an attempt to understand the flow through the renal tubule by studying the hydrodynamical aspects of an incompressible viscous fluid in a circular tube of exponentially varying cross-section with reabsorption at the wall. Following similar approach, Chandra and Prasad [7] analyzed fluid flow in rigid tube of slowly varying cross-section by considering different geometries. Also they investigated the problem by considering fluid exchange across the permeable wall governed by Starling's hypothesis. Chaturani and Ranganatha [8] studied fluid flow through a diverging/converging tube with variable wall permeability. They obtained approximate analytical solution for the case that the flux at the wall depends on wall permeability and transboundary pressure drop. Recently, Muthu and Tesfahun [9] have studied the fluid flow in nonuniform rigid wavy channel of varying cross section and presented the effects of slope parameter, reabsorption coefficient on the transverse velocity and mean pressure drop.

In all the above studies, the method used to solve the governing equations of the fluid motion is perturbation method of solution by taking small nonuniform tube parameter/curvature parameter. As per the knowledge of the authors there is no numerical study of the above problems reported in the literature.

Hence, in this paper, the Navier-Stokes equations governing the flow of an incompressible viscous fluid through a wavy (rigid diverging/converging tube of varying cross-section) non-uniform permeable tube are solved numerically by using the finite difference technique related to the method of Takabatake-Ayukawa [10]. The effects of wave number (δ), reabsorption coefficient (α), amplitude ratio (ϵ) and Reynolds number on the transverse velocity, stream function and mean pressure drop are studied without restrictions on the parameters of the problem, in principle. Further, we compared the results found by the current approach with that of perturbation method of solution.

The boundary of the tube wall vary with x . It is taken as

$$\eta(x) = d + k_1x + a \sin\left(\frac{2\pi x}{\lambda}\right), \tag{1.1}$$

where d is the radius of the tube at the inlet (at $x = 0$). k_1 is a constant whose magnitude depends on the length of the tube exit and inlet dimensions, a is the amplitude and λ is the wave length (see Fig. 1). Here, we assume $k_1 \ll 1$ to model the slowly varying slope.

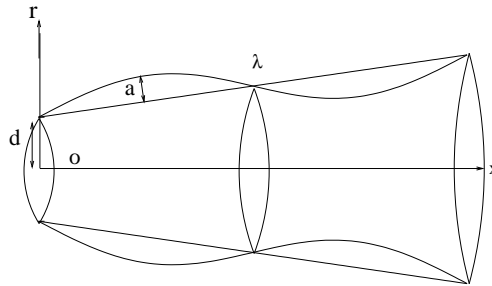


Figure 1: Geometry of the problem.

2 Mathematical formulation

Consider an incompressible fluid flow through a tube with slowly varying cross-section as given by Eq. (1.1). The motion of the fluid is assumed to be laminar, steady and symmetric. The tube is long enough to neglect the initial and end effects. The governing equations of such fluid motion are given by [6],

$$\frac{\partial u}{\partial x} + \frac{1}{r} \frac{\partial(rv)}{\partial r} = 0, \tag{2.1a}$$

$$u \frac{\partial u}{\partial x} + v \frac{\partial u}{\partial r} = -\frac{1}{\rho} \frac{\partial p}{\partial x} + \nu \left(\frac{\partial^2 u}{\partial x^2} + \frac{\partial^2 u}{\partial r^2} + \frac{1}{r} \frac{\partial u}{\partial r} \right), \tag{2.1b}$$

$$u \frac{\partial v}{\partial x} + v \frac{\partial v}{\partial r} = -\frac{1}{\rho} \frac{\partial p}{\partial r} + \nu \left[\frac{\partial^2 v}{\partial x^2} + \frac{\partial^2 v}{\partial r^2} + \frac{\partial}{\partial r} \left(\frac{v}{r} \right) \right], \tag{2.1c}$$

where u and v are the velocity components along the x and r axes respectively, p is the pressure, ρ density of the fluid and $\nu = \mu/\rho$ is kinematic viscosity.

The equations of motion are subjected to the boundary conditions:

(a) The tangential velocity at the wall is zero. That is,

$$u + \frac{d\eta}{dx}v = 0, \quad \text{at } r = \eta(x). \tag{2.2}$$

(b) The regularity condition requires

$$v = 0 \quad \text{and} \quad \frac{\partial u}{\partial r} = 0, \quad \text{at } r = 0. \tag{2.3}$$

(c) The reabsorption has been accounted for by considering the bulk flow as a decreasing function of x . That is, the flux across a cross-section is given as

$$Q(x) = \int_0^{\eta(x)} 2\pi r u(x, r) dr = Q_0 F(\alpha x), \quad (2.4)$$

where $F(\alpha x) = 1$, when $\alpha = 0$ and decreases with x , $\alpha \geq 0$ is the reabsorption coefficient and is a constant, and Q_0 is the flux across the cross-section at $x = 0$.

Introducing stream function ψ , the vorticity ω and ζ (introduced to simplify the discussion of the numerical method) by

$$u = \frac{1}{r} \frac{\partial \psi}{\partial r}, \quad v = -\frac{1}{r} \frac{\partial \psi}{\partial x}, \quad \omega = \frac{\partial v}{\partial x} - \frac{\partial u}{\partial r} \quad \text{and} \quad \zeta = r\omega, \quad (2.5)$$

and the following non-dimensional quantities

$$\begin{aligned} x' &= \frac{x}{\lambda}, & r' &= \frac{r}{d}, & \eta' &= \frac{\eta}{d}, \\ \psi' &= \frac{2\pi\psi}{Q_0}, & \alpha' &= \alpha\lambda, & \zeta' &= \frac{2\pi d^2}{Q_0} \zeta, \end{aligned}$$

the above governing equations together with boundary conditions in the dimensionless form are given by (after dropping the primes)

$$\delta^2 \frac{\partial^2 \psi}{\partial x^2} - \frac{1}{r} \frac{\partial \psi}{\partial r} + \frac{\partial^2 \psi}{\partial r^2} = -\zeta, \quad (2.6a)$$

$$\delta^2 \frac{\partial^2 \zeta}{\partial x^2} - \frac{1}{r} \frac{\partial \zeta}{\partial r} + \frac{\partial^2 \zeta}{\partial r^2} = \frac{\delta R_e}{2} \left(\frac{\partial \psi}{\partial r} \frac{\partial \zeta}{\partial x} + \frac{2}{r^2} \frac{\partial \psi}{\partial x} \zeta - \frac{\partial \psi}{\partial x} \frac{\partial \zeta}{\partial r} \right). \quad (2.6b)$$

The boundary conditions are:

$$\frac{\partial \psi}{\partial r} = \delta(k_1 + A \cos(2\pi x)) \frac{\partial \psi}{\partial x}, \quad \text{at } r = \eta(x) = 1 + kx + \epsilon \sin(2\pi x), \quad (2.7a)$$

$$\psi = 0 \quad \text{and} \quad -\frac{1}{r^2} \frac{\partial \psi}{\partial r} + \frac{1}{r} \frac{\partial^2 \psi}{\partial r^2} = 0, \quad \text{at } r = 0, \quad (2.7b)$$

$$\psi = F(\alpha x), \quad \text{at } r = \eta(x) = 1 + kx + \epsilon \sin(2\pi x), \quad (2.7c)$$

where

$$\delta = \frac{d}{\lambda}, \quad R_e = \frac{Q_0}{\pi d v}, \quad A = \frac{2\pi a}{\lambda}, \quad \epsilon = \frac{a}{d}, \quad k = \frac{k_1 \lambda}{d}.$$

The parameter R_e is the Reynolds number and δ is the wave-number (the ratio of inlet radius to the wavelength). ϵ is amplitude ratio (the ratio of amplitude to the inlet radius) and k is slope parameter. In this problem, we consider exponentially decaying bulk flow, that is, in Eq. (2.7c), F is taken as

$$F(\alpha x) = e^{-\alpha x}, \quad \text{for } 0 \leq x \leq 1. \quad (2.8)$$

3 Numerical analysis

In the present analysis, the governing equations (2.6a) and (2.6b) together with the boundary conditions (2.7a)-(2.7c) are solved numerically in the finite region ABCD (Fig. 2). Although the boundary conditions for the infinite tube have been given, the present numerical method requires furthermore the conditions on the entrance section AD and the exit section BC because the numerical analysis is carried out for the finite region ABCD as discussed by [10] and [13]. Due to this, the following conditions shall be introduced:

- a) The r -directional component of the flow velocity vanishes. That is, $v = 0$.
- b) The profile of the stream function ψ is given by the prescribed functions $f(r)$ and $g(r)$ at AD and BC respectively.

Therefore, the boundary conditions used in the analysis can be rearranged as follows:

$$\psi = 0, \quad -\frac{1}{r^2} \frac{\partial \psi}{\partial r} + \frac{1}{r} \frac{\partial^2 \psi}{\partial r^2} = 0, \quad \text{on AB,} \quad (3.1a)$$

$$\psi = f(r), \quad \frac{\partial \psi}{\partial x} = 0, \quad \text{on AD (inflow),} \quad (3.1b)$$

$$\psi = Q_0 e^{-\alpha x}, \quad \frac{\partial \psi}{\partial r} = \delta(k_1 + A \cos(2\pi x)) \frac{\partial \psi}{\partial x}, \quad \text{on CD,} \quad (3.1c)$$

$$\psi = g(r), \quad \frac{\partial \psi}{\partial x} = 0, \quad \text{on BC (outflow),} \quad (3.1d)$$

where $f(r)$ and $g(r)$ are functions of r , such that u is parabolic at AD and BC sections. We assume that these functions satisfy the boundary conditions so that the solution is free from discontinuities.

The finite region ABCD is divided by an integral number of meshes N in the x -direction and by an integral number of meshes M in the r -direction, thus the lattice points are numbered i and j . Then the mesh sizes in x and r -direction are given re-

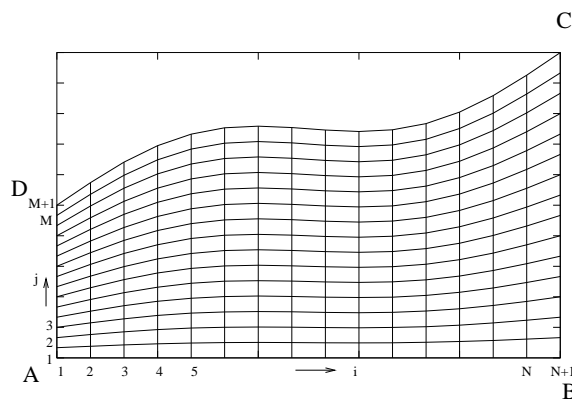


Figure 2: Calculating region of the problem.

spectively by

$$k = \frac{1}{N}, \quad h_i = \frac{\eta(x_i)}{M}, \quad \text{with } \eta(x_i) = 1 + kx_i + \epsilon \sin(2\pi x_i). \quad (3.2)$$

3.1 Finite difference approximation of the governing equations

Consider six lattice points $(x, r), (x + k, r + \delta_{i,j}), (x, r + h_i), (x - k, r - \delta_{i-1,j}), (x, r - h_i), (x - k, r - h_{i-1} - \delta_{i-1,j})$ numbered 0, 1, 2, 3, 4, 5 respectively in Fig. 3, and try to determine the coefficients α_n so that the following difference equation is satisfied:

$$\left(\delta^2 \frac{\partial^2 \psi}{\partial x^2} - \frac{1}{r} \frac{\partial \psi}{\partial r} + \frac{\partial^2 \psi}{\partial r^2} \right) \Big|_0 = \alpha_0 \psi_0 + \alpha_1 \psi_1 + \alpha_2 \psi_2 + \alpha_3 \psi_3 + \alpha_4 \psi_4 + \alpha_5 \psi_5, \quad (3.3)$$

where ψ_n represents the value of function ψ at the point numbered n .

By expanding each ψ_n in Eq. (3.3) by Taylor series about the point numbered 0 and equating the coefficients of ψ_n , we get a set of equations for the unknown terms α_n . Then substituting Eq. (3.3) into Eq. (2.6a) yields the following ψ difference equation with a second order accuracy $o(h^2, k^2)$ when centred differences are used, which is based on Eq. (2.6a), can be written as

$$\alpha_0 \psi_{i,j} + \alpha_1 \psi_{i+1,j} + \alpha_2 \psi_{i,j+1} + \alpha_3 \psi_{i-1,j} + \alpha_4 \psi_{i,j-1} + \alpha_5 \psi_{i-1,j-1} + \zeta_{i,j} = 0, \quad (3.4)$$

where

$$\begin{aligned} \alpha_0 &= \frac{-2}{h_i^2} - \frac{\delta^2}{k^2} (2 + D_{i,j}), & \alpha_1 &= \frac{\delta^2}{k^2}, \\ \alpha_2 &= \frac{1}{h_i^2} - \frac{1}{2r_{i,j}h_i} + \frac{\delta^2}{2k^2} (D_{i,j} - 2K_{i,j}), & \alpha_3 &= \frac{\delta^2}{k^2} (1 + R_{i,j}), \\ \alpha_4 &= \frac{1}{h_i^2} + \frac{1}{2r_{i,j}h_i} + \frac{\delta^2}{2k^2} (D_{i,j} + 2K_{i,j}), & \alpha_5 &= -\frac{\delta^2}{k^2} R_{i,j}, \\ D_{i,j} &= S_{i,j}^2 + \frac{h_{i-1}}{h_i} S_{i,j} - 2K_{i,j}^2, & S_{i,j} &= \frac{\delta_{i,j} + \delta_{i-1,j}}{h_i}, \\ K_{i,j} &= \frac{\delta_{i,j}}{h_i}, & R_{i,j} &= \frac{\delta_{i,j} + \delta_{i-1,j}}{h_{i-1}}. \end{aligned}$$

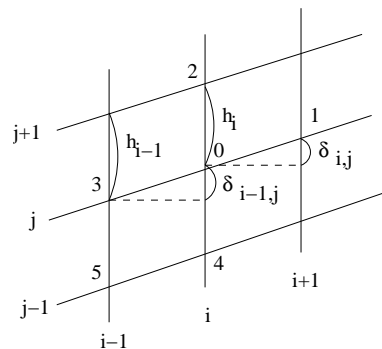


Figure 3: Lattice points on the interior region.

Substituting Eq. (3.3) into Eq. (2.6b), we obtain a difference equation with respect to ζ . The approximations to the derivatives $\partial\zeta/\partial x$ and $\partial\zeta/\partial r$ are carried out by applying the up-wind difference technique, which is superior in stability for non-linear terms and is fast in convergence of the calculation [10]. We set

$$\beta = \psi_1 - \psi_3, \quad \gamma = \psi_2 - \psi_4,$$

and decide the stream direction from signs of β and γ . Then, to assure the dominance of the coefficient of ω_0 , the center point numbered 0 and the points in the up-stream are used in the difference approximations to $\partial\zeta/\partial x$ and $\partial\zeta/\partial r$. Then we obtain

$$\begin{aligned} \frac{\partial\zeta}{\partial x}\Big|_0 &= \frac{1}{k}(\zeta_0 - \zeta_3 - (\zeta_2 - \zeta_0)\frac{\delta_{i-1,j}}{h_i}), & \frac{\partial\zeta}{\partial r}\Big|_0 &= \frac{\zeta_2 - \zeta_0}{h_i}, & \beta \geq 0, \quad \gamma \geq 0, \\ \frac{\partial\zeta}{\partial x}\Big|_0 &= \frac{1}{k}(\zeta_1 - \zeta_0 - (\zeta_2 - \zeta_0)K_{i,j}), & \frac{\partial\zeta}{\partial r}\Big|_0 &= \frac{\zeta_2 - \zeta_0}{h_i}, & \beta \geq 0, \quad \gamma < 0, \\ \frac{\partial\zeta}{\partial x}\Big|_0 &= \frac{1}{k}(\zeta_0 - \zeta_3 - (\zeta_0 - \zeta_4)\frac{\delta_{i-1,j}}{h_i}), & \frac{\partial\zeta}{\partial r}\Big|_0 &= \frac{\zeta_0 - \zeta_4}{h_i}, & \beta < 0, \quad \gamma \geq 0, \\ \frac{\partial\zeta}{\partial x}\Big|_0 &= \frac{1}{k}(\zeta_1 - \zeta_0 - (\zeta_0 - \zeta_4)K_{i,j}), & \frac{\partial\zeta}{\partial r}\Big|_0 &= \frac{\zeta_0 - \zeta_4}{h_i}, & \beta < 0, \quad \gamma < 0. \end{aligned}$$

Consequently, the ζ difference equations are obtained as follows:

$$\beta_0\zeta_{i,j} + \beta_1\zeta_{i+1,j} + \beta_2\zeta_{i,j+1} + \beta_3\zeta_{i-1,j} + \beta_4\zeta_{i,j-1} + \beta_5\zeta_{i-1,j-1} = 0, \tag{3.5}$$

where

$$\beta_0 = r_{i,j}\alpha_0 + \frac{\delta R_e}{4kh_i} \left(-|\beta| - |\gamma| + \text{sgn}(\beta)\text{sgn}(\gamma)\frac{1}{2}\gamma T_{i,j} - \frac{2h_i}{r_{i,j}} \left(\beta - \gamma\frac{1}{2}S_{i,j} \right) \right),$$

$$\beta_1 = r_{i,j}\alpha_1 + \frac{\delta R_e}{4kh_i} \gamma (H(\gamma) - 1),$$

$$\beta_2 = r_{i,j}\alpha_2 + \frac{\delta R_e}{4kh_i} \left(|\beta| - \text{sgn}(\beta)\text{sgn}(\gamma)\frac{1}{2}\gamma T_{i,j} \right) H(\beta),$$

$$\beta_3 = r_{i,j}\alpha_3 + \frac{\delta R_e}{4kh_i} \gamma H(\gamma),$$

$$\beta_4 = r_{i,j}\alpha_4 + \frac{\delta R_e}{4kh_i} \left(-|\beta| + \text{sgn}(\beta)\text{sgn}(\gamma)\frac{1}{2}\gamma T_{i,j} \right) (H(\beta) - 1),$$

$$\beta_5 = r_{i,j}\alpha_5,$$

$$H(x) = \begin{cases} 1, & \text{if } x \geq 0, \\ 0, & \text{if } x < 0, \end{cases} \quad \text{sgn}(x) = \begin{cases} 1, & \text{if } x > 0, \\ 0, & \text{if } x = 0, \\ -1, & \text{if } x < 0, \end{cases} \quad \text{and} \quad T_{i,j} = \frac{\delta_{i,j} - \delta_{i-1,j}}{h_i}.$$

3.2 Finite difference approximation on the boundaries

In this section, we develop difference approximations to Eq. (2.6a) on the boundaries. We consider the four points on and near the boundary AB, numbered 0, 1, 2, 3 respectively, as shown in Fig. 4, and try to determine the coefficients a_n ,

$$\left(\delta^2 \frac{\partial^2 \psi}{\partial x^2} - \frac{1}{r} \frac{\partial \psi}{\partial r} + \frac{\partial^2 \psi}{\partial r^2} \right) \Big|_0 = a_0\psi_0 + a_1\psi_1 + a_2\psi_2 + a_3\psi_3 + a_4 \left(-\frac{1}{r^2} \frac{\partial \psi}{\partial r} + \frac{1}{r} \frac{\partial^2 \psi}{\partial r^2} \right) \Big|_0. \tag{3.6}$$

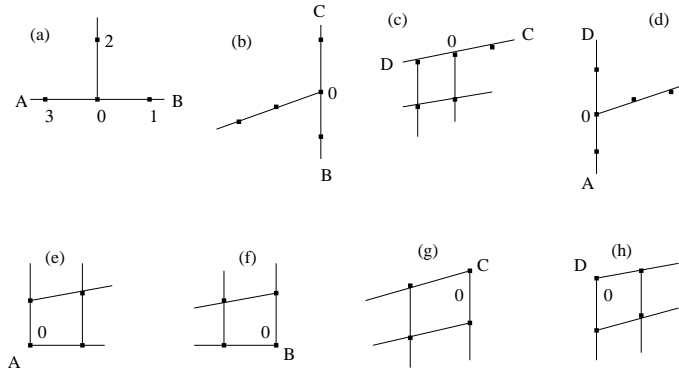


Figure 4: Lattice points on the boundaries.

Similar to the method used to find α_n , we can easily obtain a difference equation on the boundary AB. Applying the boundary equation (3.1) to this difference equation $\zeta_{i,j}$ on AB is found as

$$\zeta_{i,j} = 0, \quad \text{on AB } (i = 2, \dots, N, j = 1). \tag{3.7}$$

Similarly on and near the boundaries BC, CD, AD, we consider the five points shown in Fig. 4. Then the difference equations are approximated by using ψ at these five points and $\partial\psi/\partial x$ or $\partial\psi/\partial r$ at the point numbered 0. At the points A, B, C, D, we consider the four points shown in Fig. 4. Then the difference equations are approximated by using ψ at these four points and $\partial\psi/\partial x$ and $-r^{-2}\partial\psi/\partial r + r^{-1}\partial^2\psi/\partial r^2$ at the point numbered 0. By applying the boundary conditions (3.1) to these difference equations, $\zeta_{i,j}$ on each boundary can be expressed as

$$\zeta_{i,j} = b_0\psi_{i,j} + b_1\psi_{i,j-1} + b_2\psi_{i+1,j} + b_3\psi_{i+2,j} + b_4\psi_{i,j+1}, \quad \text{on AD } (i = 1, j = 2, \dots, M), \tag{3.8}$$

where

$$b_0 = \frac{2}{h_1^2} + \frac{\delta^2}{k^2} \left[\frac{S_{2,j} + K_{2,j}}{T_{2,j}} + K_{1,j}R_{2,j} \right], \quad b_2 = -2 \frac{\delta^2}{k^2} \frac{S_{2,j}}{T_{2,j}}, \tag{3.9a}$$

$$b_1 = \frac{-1}{h_1^2} - \frac{1}{2r_{1,j}h_1} - \frac{\delta^2}{2k^2} K_{1,j}R_{2,j} \left[\frac{h_1}{h_2} \frac{1}{T_{2,j}} + 1 \right], \quad b_3 = \frac{\delta^2}{k^2} \frac{h_1}{h_2} \frac{K_{1,j}}{T_{2,j}}, \tag{3.9b}$$

$$b_4 = \frac{-1}{h_1^2} + \frac{1}{2r_{1,j}h_1} - \frac{\delta^2}{2k^2} K_{1,j}R_{2,j} \left[1 - \frac{h_1}{h_2} \frac{1}{T_{2,j}} \right], \tag{3.9c}$$

$$\zeta_{i,j} = c_0\psi_{i,j} + c_1\psi_{i,j+1} + c_2\psi_{i-1,j} + c_3\psi_{i-2,j} + c_4\psi_{i,j-1}, \quad \text{on BC } (i = N + 1, j = 2, \dots, M), \tag{3.9d}$$

where

$$c_0 = \frac{2}{h_{N+1}^2} + \frac{\delta^2}{k^2} \left[-\frac{h_{N-1}}{h_N} \left(\frac{R_{N,j} + K_{N-1,j}}{T_{N,j}} \right) + \left(\frac{h_N}{h_{N+1}} \right)^2 K_{N,j}S_{N,j} \right], \tag{3.10a}$$

$$c_1 = \frac{-1}{h_{N+1}^2} + \frac{1}{2r_{N+1,j}h_{N+1}} - \frac{\delta^2}{2k^2} \frac{h_N}{h_{N+1}} K_{N,j}S_{N,j} \left[\frac{h_N}{h_{N+1}} - \frac{1}{T_{N,j}} \right], \tag{3.10b}$$

$$c_2 = 2 \frac{\delta^2 S_{N,j}}{k^2 T_{N,j}}, \quad c_3 = -\frac{\delta^2 K_{N,j}}{k^2 T_{N,j}}, \tag{3.10c}$$

$$c_4 = \frac{-1}{h_{N+1}^2} - \frac{1}{2r_{N+1,j}h_{N+1}} - \frac{\delta^2 h_N}{2k^2 h_{N+1}} K_{N,j} S_{N,j} \left[\frac{h_N}{h_{N+1}} + \frac{1}{T_N} \right], \tag{3.10d}$$

$$\zeta_{i,j} = e_1 \psi_{i,j} + e_2 \psi_{i-1,j} + e_3 \psi_{i-1,j-1} + e_4 \psi_{i,j-1} + e_5 \psi_{i+1,j}, \quad \text{on CD } (i = 2, \dots, N, j = M + 1), \tag{3.10e}$$

where

$$\begin{aligned} e_1 &= \frac{2}{h_i^2} + \frac{\delta^2}{k^2} (2 + D_{i,M+1}) + \frac{2\delta}{h_i k} - \frac{\delta}{r_{i,j} k} + \frac{\delta^3}{k^3} (h_i D_{i,M+1} - 2\delta_{i,M+1}) (k_1 \\ &\quad + A \cos(2\pi x)) \frac{\delta_{i,M+1} + \delta_{i-1,M+1}}{\delta_{i-1,M+1} - \delta_{i,M+1}}, \\ e_2 &= -\frac{\delta^2}{k^2} (1 + R_{i,M+1}) - \frac{2\delta}{h_i k} + \frac{\delta}{r_{i,j} k} - \frac{\delta^3}{k^3} (h_i D_{i,M+1} - 2\delta_{i,M+1}) (k_1 \\ &\quad + A \cos(2\pi x)) \frac{\delta_{i,M+1}}{\delta_{i-1,M+1} - \delta_{i,M+1}}, \\ e_3 &= \frac{\delta^2}{k^2} R_{i,M+1}, \quad e_4 = -\frac{2}{h_i^2} - \frac{\delta^2}{k^2} D_{i,M+1}, \\ e_5 &= -\frac{\delta^2}{k^2} - \frac{2\delta}{h_i k} + \frac{\delta}{r_{i,j} k} - \frac{\delta^3}{k^3} (h_i D_{i,M+1} - 2\delta_{i,M+1}) (k_1 \\ &\quad + A \cos(2\pi x)) \frac{\delta_{i-1,M+1}}{\delta_{i-1,M+1} - \delta_{i,M+1}}. \end{aligned}$$

At the corner points

$$\zeta_{i,j} = 0, \quad \text{on A } (i = 1, j = 1), \tag{3.11a}$$

$$\zeta_{i,j} = 0, \quad \text{on B } (i = N + 1, j = 1), \tag{3.11b}$$

$$\zeta_{i,j} = d_0 \psi_{i,j} + d_1 \psi_{i,j-1} + d_2 \psi_{i+1,j-1} + d_3 \psi_{i+1,j}, \quad \text{on D } (i = 1, j = M + 1), \tag{3.11c}$$

where

$$d_0 = \frac{2}{h_i^2} + 2 \frac{\delta^2}{k^2} \left(1 - \frac{h_2}{h_1} K_{1,M+1} + K_{1,M+1}^2 \right), \quad d_1 = \frac{-2}{h_i^2} - 2 \frac{\delta^2}{k^2} K_{1,M+1} \left(K_{1,M+1} - \frac{h_2}{h_1} \right), \tag{3.12a}$$

$$d_2 = -2 \frac{\delta^2 h_1}{k^2 h_2} K_{1,M+1}, \quad d_3 = 2 \frac{\delta^2}{k^2} \left(K_{1,M+1} \frac{h_1}{h_2} - 1 \right), \tag{3.12b}$$

$$\zeta_{i,j} = f_1 \psi_{i,j} + f_2 \psi_{i,j-1} + f_3 \psi_{i-1,j-1} + f_4 \psi_{i-1,j}, \quad \text{on C } (i = N + 1, j = M + 1), \tag{3.12c}$$

where

$$f_1 = \frac{2}{h_{N+1}^2} + 2 \frac{\delta^2}{k^2} \left(1 + \frac{h_N^2}{h_{N+1}^2} K_{N,M+1} (1 + K_{N,M+1}) \right), \quad f_3 = 2 \frac{\delta^2}{k^2} K_{N,M+1},$$

$$f_2 = -\frac{2}{h_{N+1}^2} - 2 \frac{\delta^2}{k^2} \frac{h_N^2}{h_{N+1}^2} K_{N,M+1} (1 + K_{N,M+1}), \quad f_4 = -2 \frac{\delta^2}{k^2} (1 + K_{N,M+1}).$$

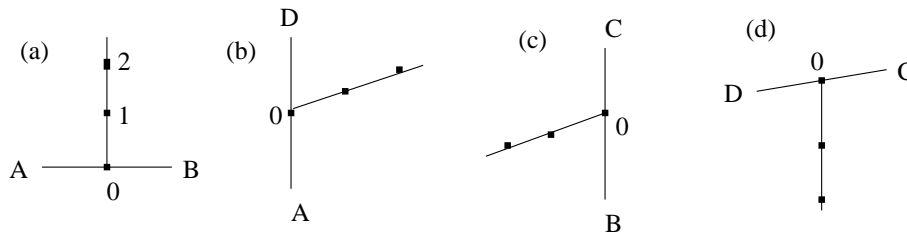


Figure 5: Lattice points on the boundaries.

Finally, when we consider the three points on and near the boundary AB shown by Fig. 5, the derivatives of ψ can be approximated by

$$-\frac{1}{r^2} \frac{\partial \psi}{\partial r} + \frac{1}{r} \frac{\partial^2 \psi}{\partial r^2} = \frac{1}{2h_i r^2} (\psi_2 - 4\psi_1 + 3\psi_0).$$

Then, by using the boundary condition (3.1), we obtain

$$\psi_{i,j} = \frac{1}{4} \psi_{i,j+1}, \quad \text{on AB } (i = 2, \dots, N, j = 2). \tag{3.13}$$

Similarly the following formulas are obtained for other boundaries.

$$\psi_{i,j} = \frac{\delta_{i,j} \psi_{i-1,j} + \delta_{i-1,j} \psi_{i+1,j}}{\delta_{i-1,j} + \delta_{i,j}}, \quad \text{on AD } (i = 2, j = 2, \dots, M), \tag{3.14a}$$

$$\psi_{i,j} = \frac{\delta_{N,j} \psi_{i-1,j} + \delta_{N-1,j} \psi_{i+1,j}}{\delta_{N-1,j} + \delta_{N,j}}, \quad \text{on BC } (i = N, j = 2, \dots, M), \tag{3.14b}$$

$$\psi_{i,j} = \frac{1}{4} (3\psi_{i,j+1} + \psi_{i,j-1} - 2h_i \delta(k_1 + A \cos(2\pi x)) f_0), \quad \text{on DC } (i = 2, \dots, N, j = M), \tag{3.14c}$$

where

$$f_0 = \frac{((\delta_{i,M+1} + \delta_{i-1,M+1})\psi_{i,j+1} - \delta_{i,M+1}\psi_{i-1,j+1} - \delta_{i-1,M+1}\psi_{i+1,j+1})}{k(\delta_{i,M+1} - \delta_{i-1,M+1})}.$$

The computational procedure to calculate ψ and ζ on the region ABCD and the values of parameters related to SOR method are similar to the one given by Takabatake and Ayukawa [10].

Now, the nondimensional pressure $p(x, r)$ can be obtained by using Eq. (2.1b) and ψ which is found by difference approximation. It is given as

$$p(x, r) = \delta \frac{\partial u}{\partial x} + \frac{1}{\delta} \int \frac{\partial^2 u}{\partial r^2} dx + \frac{1}{\delta} \int \frac{1}{r} \frac{\partial u}{\partial r} dx - \frac{R_e}{2} \left(\int u \frac{\partial u}{\partial x} dx + \int v \frac{\partial u}{\partial y} dx \right). \tag{3.15}$$

The mean pressure is given as

$$\bar{p}(x) = \frac{1}{\pi \eta^2(x)} \int_0^{\eta(x)} 2\pi r p(x, r) dr. \tag{3.16}$$

Further, the mean pressure drop between $x = 0$ and $x = x_0$ is calculated using

$$\Delta \bar{p}(x_0) = \bar{p}(0) - \bar{p}(x_0). \tag{3.17}$$

4 Results and discussion

In the present calculation, the integral numbers of meshes are set as $M = N = 15$. First, we performed the calculation for the velocity profile and compared with the analytical results based upon the perturbation method. They were in good agreement and are given in Fig. 6(a) and (b). It is found that the maximum difference between the two approaches is 2.2×10^{-1} .

In order to assess the effects of grid dependence on the numerical solution, computations are conducted on two sets of grids, i.e., 15×15 and 16×16 cell meshes. Fig. 7 compares the computed mean pressure drop variation in the axial direction obtained by using the numerical method on these grids and shows the effect of grid size on the computed results. As the differences are negligible most of the computations reported from this point onwards are done using the 15×15 grid size.

The objective of this analysis is to study the behavior of an incompressible fluid flow through a tube of converging/diverging and slowly varying cross-section with

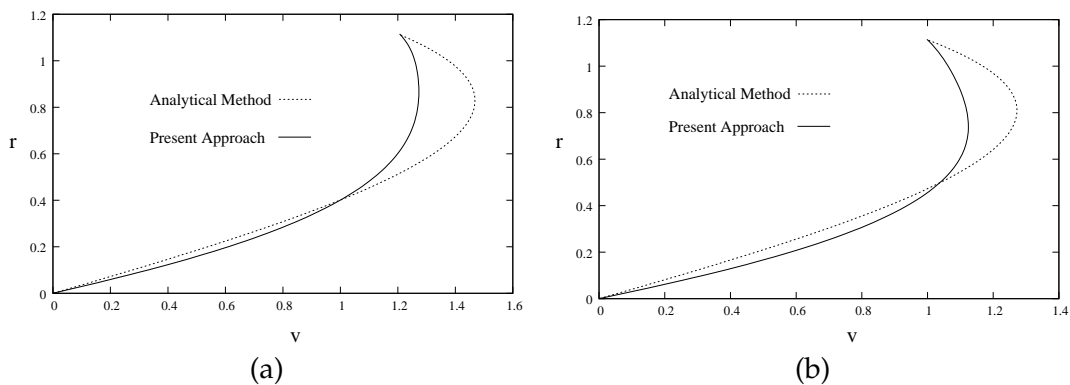


Figure 6: (a) Comparison of transverse velocity between Analytical method and numerical approach ($\alpha = 2.0$); (b) Comparison of transverse velocity for between Analytical method and numerical approach ($\alpha = 1.5$).

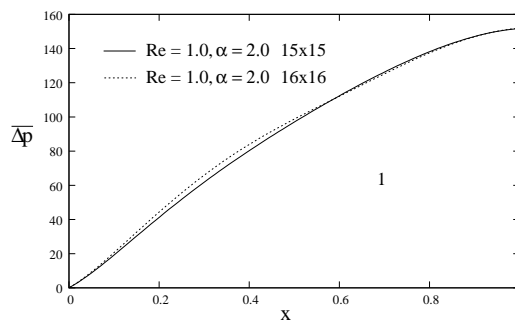


Figure 7: Grid dependence studies on two set of grids.

absorbing walls by numerical approach. It may be recalled that k characterize the slope of the converging/diverging wavy walls. $k = 1.0$ represents a diverging tube, $k = 0$ represents a normal (sinusoidal) tube and $k = -1.0$ represents a converging tube. ϵ and α represents amplitude and reabsorption coefficient of wavy walls.

We discuss the effects of these parameters on the radial velocity ($v(x, r)$), mean pressure drop ($\Delta\bar{p}(x)$) and stream function $\psi(x, r)$. In all our numerical calculations, the following parameters are fixed as $A = 0.0628$, $\delta = 0.1$ and $\epsilon = 0.1$.

4.1 The velocity v

The velocity field can be obtained from difference approximation of the stream function. In this section, we discuss the effects of the slope parameter (k), reabsorption coefficient (α) and Reynolds number on the radial velocity.

The effect of slope parameter (k) on the radial velocity is shown in Fig. 8. The velocity is more for divergent tube than the normal (sinusoidal) tube, and it is less for convergent tube than the other two. Fig. 9 illustrates the effect of Reynolds number on the velocity v versus r . As shown, the Reynolds number produces significant influence on the radial velocity. As Re increases from 1 to 5, the velocity increases and the point where the velocity attains its maximum decreases from $\cong 0.6$ to $\cong 0.4$.

The effect of reabsorption coefficient α is presented in the Figs. 10(a), (b) and (c). It

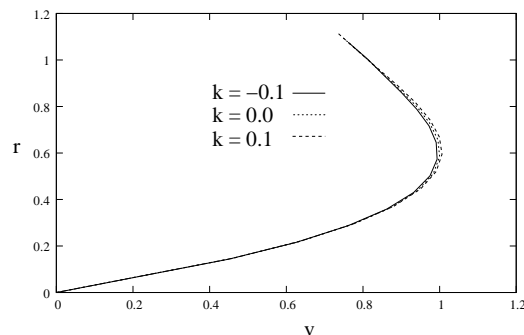


Figure 8: Distribution of transverse velocity (v) with y ($Re = 1.0$, $\alpha = 1.0$, $x = 0.2$).

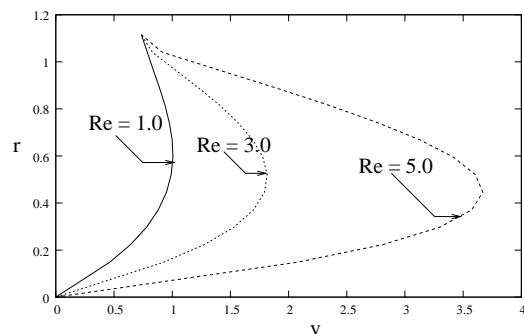


Figure 9: Distribution of transverse velocity (v) with y ($k = 0.1$, $\alpha = 1.0$, $x = 0.2$).

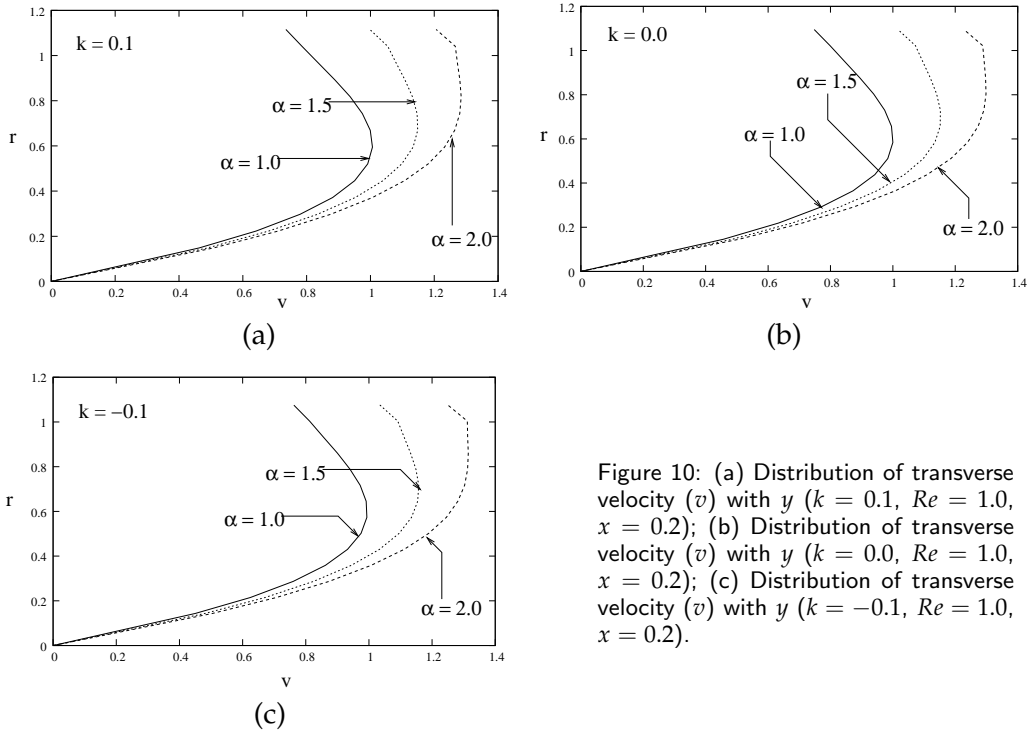


Figure 10: (a) Distribution of transverse velocity (v) with y ($k = 0.1, Re = 1.0, x = 0.2$); (b) Distribution of transverse velocity (v) with y ($k = 0.0, Re = 1.0, x = 0.2$); (c) Distribution of transverse velocity (v) with y ($k = -0.1, Re = 1.0, x = 0.2$).

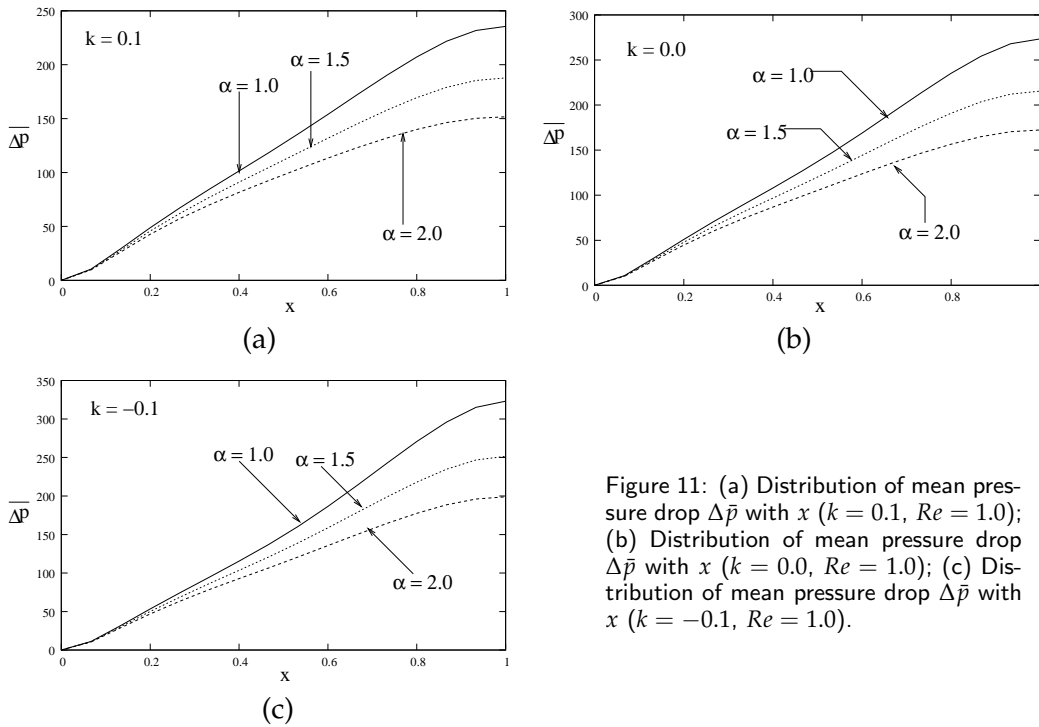


Figure 11: (a) Distribution of mean pressure drop $\Delta \bar{p}$ with x ($k = 0.1, Re = 1.0$); (b) Distribution of mean pressure drop $\Delta \bar{p}$ with x ($k = 0.0, Re = 1.0$); (c) Distribution of mean pressure drop $\Delta \bar{p}$ with x ($k = -0.1, Re = 1.0$).

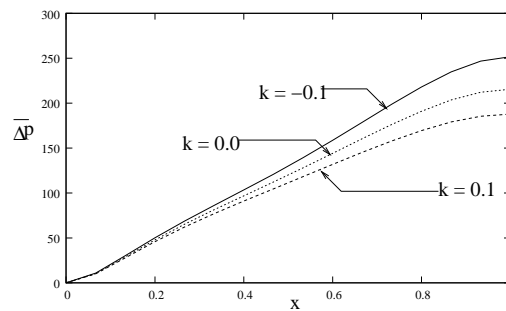


Figure 12: Distribution of mean pressure drop $\Delta\bar{p}$ with x ($Re = 1.0$, $\alpha = 1.5$).

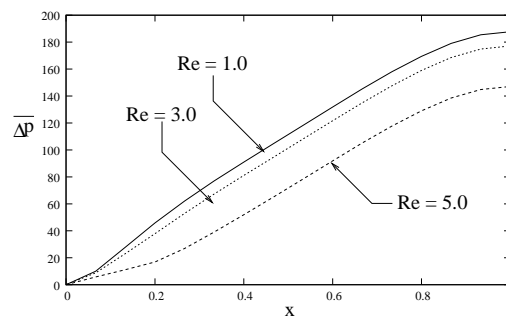


Figure 13: Distribution of mean pressure drop $\Delta\bar{p}$ with x ($k = 0.1$, $\alpha = 1.5$).

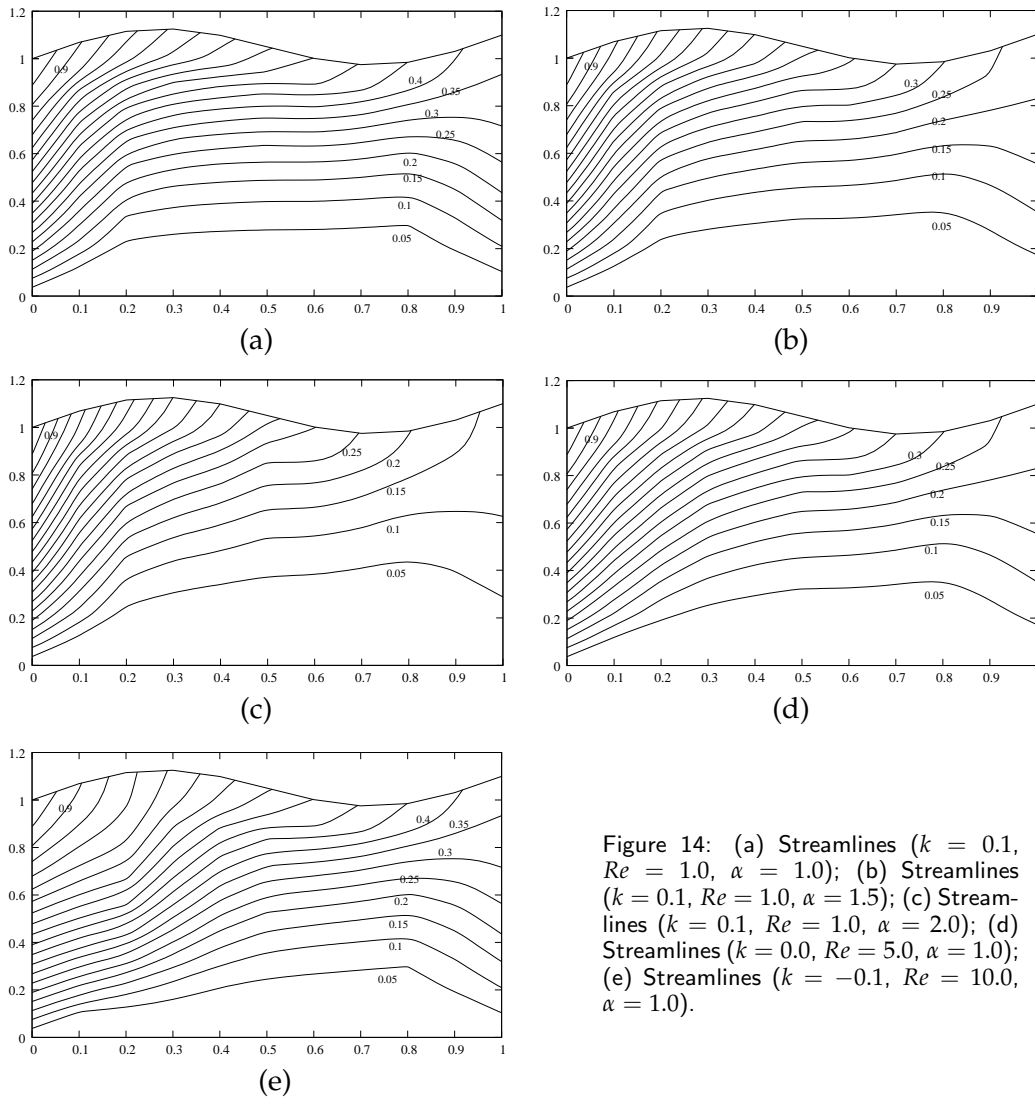
can be observed from the figures that as α increases, the transverse velocity of the flow increases for all cases (converging, normal, and diverging tubes).

4.2 Mean pressure drop $\Delta\bar{p}$

The values of the mean pressure drop (Eq. (3.17)) over the length of the tube are calculated for different values of k , Re and α . As shown, in Figs. 11(a), (b) and (c), when the reabsorption coefficient α increases, the mean pressure drop decrease for all three forms of the tube (convergent, normal and divergent tubes). Fig. 12 displays the effect of slope parameter k to mean pressure drop. We can notice that $\Delta\bar{p}$ is less for the divergent tube than the normal or convergent tubes, and it is more for convergent tube than the normal/divergent tubes. Fig. 13 shows the influence of Reynolds number Re on $\Delta\bar{p}$. The value of the mean pressure drop $\Delta\bar{p}$ decreases as Re increases.

4.3 Stream function

We can observe the flow behavior of the fluid by looking at the contour drawing of the stream function for various values of reabsorption coefficient α and for the Reynolds number Re . Figs. 14(a), (b) and (c) shows the effect of α on the flow behavior of the fluid. It can be observed that as α increases, the stream lines moves to the boundary because of more absorption. Figs. 14(a), (d) and (e) are showing the flow pattern when Re increases.



5 Conclusions

In the present study, an analysis of mathematical model of incompressible fluid flow in a rigid tube of slowly varying converging/diverging walls has been presented with possible applications to the flow of fluid in renal tubules. The main contribution of this study is to use the numerical method to solve the Navier-Stock equations for an incompressible, steady, viscous flow without imposing any restriction on the parameters of the problem. The reabsorption coefficient α , the slope parameter k and the Reynolds number Re have the same effect on the radial velocity. As they increases, the velocity also increases. The mean pressure drop decreases for rise of reabsorption coefficient for all three forms of the tube (converging, normal (sinusoidal) and diverging

tubes). It is also less for the divergent tube than the normal or convergent tubes, and it is more for convergent tube than the normal/divergent tubes. The streamlines shows the general trend of the fluid flow. Physically, as the reabsorption coefficient increases the fluid that come out of the tube becomes less.

References

- [1] R. I. MACEY, *Pressure flow patterns in a cylinder with reabsorbing walls*, Bull. Math. Biophys., 25 (1963), pp. 1–9.
- [2] R. B. KELMAN, *A theoretical note on exponential flow in the proximal part of the mammalian nephron*, Bull. Math. Biophys., 24 (1962), pp. 31–38.
- [3] R. I. MACEY, *Hydrodynamics in renal tubules*, Bull. Math. Biophys., 27 (1965), pp. 117–124.
- [4] E. A. MARSHALL AND E. A. TROWBRIDGE, *Flow of a Newtonian fluid through a permeable tube: the application to the proximal renal tubule*, Bull. Math. Bio., 36 (1974), pp. 457–476.
- [5] P. J. PALATT, H. SACKIN AND R. TANNER, *A hydrodynamical model of a permeable tubule*, J. Theor. Biol., 44 (1974), pp. 287–303.
- [6] G. RADHAKRISHNAMACHARYA, P. CHANDRA AND M. R. KAIMAL, *A hydrodynamical study of the flow in renal tubules*, Bull. Math. Bio., 43(2) (1981), pp. 151–163.
- [7] P. CHANDRA AND J.S.V.R. KRISHNA PRASAD, *Low reynolds number flow in tubes of varying cross-section with absorbing walls*, J. Math. Phys. Sci., 26(1) (1992), pp. 19–36.
- [8] P. CHATURANI AND T. R. RANGANATHA, *Flow of Newtonian fluid in non-uniform tubes with variable wall permeability with application to flow in renal tubules*, Acta. Mech., 88 (1991), pp. 11–26.
- [9] P. MUTHU AND T. BERHANE, *Mathematical model of flow in renal tubules*, Int. Jr. App. Math. Mech., 6 (20) (2010), pp. 94–107.
- [10] S. TAKABATAKE AND K. AYUKAWA, *Numerical study of two-dimensional peristaltic flows*, J. Fluid. Mech., 122 (1982), pp. 439–465.
- [11] K. AYUKAWA AND S. TAKABATAKE, *Numerical analysis of two-dimensional peristaltic flows*, Bull. JSME., 25 (1982), pp. 1061–1069.
- [12] S. TAKABATAKE, K. AYUKAWA AND A. MORI, *Peristaltic pumping in circular cylindrical tubes: a numerical study of fluid transport and its efficiency*, J. Fluid. Mech., 193 (1988), pp. 267–283.
- [13] E. F. ELSHEHAWAY, E. M. E. ELBARBARY AND N. S. ELGAZERY, *Effect of inclined magnetic field on magneto fluid flow through a porous medium between two inclined wavy porous plates (numerical study)*, Appl. Math. Comput., 135 (2003), pp. 85–103.